Proceedings of the 2002 IEEE
International Conference on Robotics & Automation
Washington, DC • May 2002

Two-Time Scale Shape Control of Flexible Payloads Grasped by Actuated Grippers

Edward J. Park[1], Bongsoo Kang[1,2] and James K. Mills[1]

[1]University of Toronto, Toronto, Canada, epark@mie.utoronto.ca, mills@mie.utoronto.ca
[2]Hannam University, Taejon, Korea, bskang@mail.hannam.ac.kr

Abstract

This paper presents a theoretical framework to simultaneously control both static shape deformation and vibration of a flexible payload grasped by an actuated robotic gripper. The dynamic model of the actuated flexible payload is derived using the component mode synthesis (CMS) method with addition of quasi-static modes. Then, the dynamic component model is used to synthesize a simultaneous static shape and vibration controller. Two-time scale control scheme is pursued taking advantage of the two-time scale behavior between the quasi-static modes and vibration modes, which are employed in the model. Simulation results demonstrate the effectiveness of the proposed control approach to simultaneously correct static deformation and suppress vibration in the payload.

1. Introduction

Interest in robotic manipulation of flexible payloads has grown recently due to its potential application to many assembly processes in industries. Especially in the aircraft and automotive industries, use of robotic technology has the potential to improve the current assembly technology of flexible thin-walled payloads, such as sheet metal parts. Assembly of these parts with robots replacing costly fixtures has potential cost savings. For such application to the automotive industry, see [1].

One of the major problems in robotic manipulation of flexible payloads is to maintain a desired shape of the payload, while suppressing its vibration during assembly. The structural flexibility of these payloads creates difficulties in ensuring mating surfaces and contact points are properly aligned for successful assembly. Gravity causes the part to statically deform under its own weight. In contrast, robot motion induced vibration leaves the shape of the part unchanged once the vibration is damped out. However, since subsequent assembly operations are delayed until the vibration decays, reduction of the vibration settling time is critical for high-speed assembly. To the best of our knowledge, work reported in the literature has addressed vibration control of flexible payloads, but has not dealt with simultaneous vibration, and static deformation. To satisfy typical assembly position tolerance requirements, gravity-induced static deformation of flexible parts cannot be ignored.

In order to solve both the static deformation and vibration problems, we propose an actuated robotic gripper, which is configured with discrete (or "point") linear actuators and position sensors. Such a gripper will be capable of actively modifying the static and dynamic responses of the flexible payload simultaneously. Figure 1 shows a schematic of the gripper. The robot and the gripper structures are considered to be rigid, while the flexible payload exhibits elastic deflections.

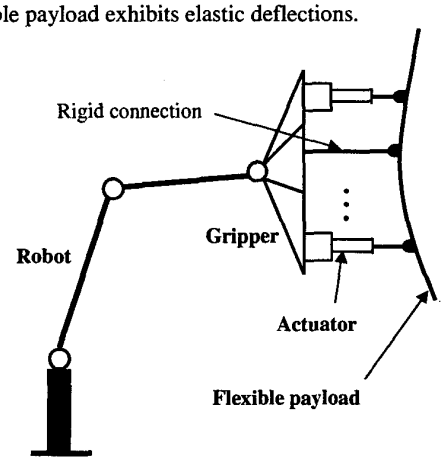

Fig. 1 Actuated robotic gripper holding a flexible payload

The purpose of this paper is to present an effective control design approach for shape control of a flexible payload grasped by an actuated robotic gripper. The aim of the shape control is to correct static shape deformation and suppress vibration in the payload simultaneously. The approach pursued here starts with the component mode synthesis (CMS) formulation of the actuated flexible payload with inclusion of quasi-static modes, which was proposed and studied in our previous paper [12]. Based on the component model, a two-time scale model is derived. This allows the definition of a slow subsystem corresponding to the quasi-static motions and a fast subsystem corresponding to the vibration motions. Then a composite controller, consisting of slow and fast controls for the quasi-static and vibration motions, respectively, is designed separately.

Note that the CMS method allows the explicit expression of coupling dynamics between the flexible payload and the gripper actuators, while reducing the order of the dynamic model for control design. In this study, the constraint modes, vibration normal modes and quasi-static modes are selected as the component mode sets. In our previous paper [12], it was found that the inclusion of these three types modes results in higher

accuracy simulation of dynamic responses of the flexible payload, subject to both static and dynamic external forces. The use of constraint modes allows better representation of the effects of the actuators on the flexible payload [2]. Vibration normal modes contain correct frequency information when the frequency of external forcing is near or higher than the first natural frequency of the flexible payload [4]. The quasi-static modes bear correct frequency information when the frequency of external forcing is much lower than the first natural frequency of the flexible payload [3]. The two-time scale modeling then takes advantage of the two-time scale behavior between the quasi-static modes and vibration modes, to synthesize a compact controller.

The main contribution of this work is to address the problem of simultaneously controlling static shape deformation and vibration of a flexible payload. A numerical example is presented using a flexible sheet metal plate. The simulation results validate the theoretical conclusions. The results of this paper maybe applied to a general problem that requires simultaneous control of both static and dynamic elastic deflections.

This paper is organized as follows. In the next section, the CMS formulation is described. Section 3 derives two-time scale models. Section 4 and 5 presents composite modal controller and two-time scale modal estimator, respectively. Section 6 gives simulation results. Finally, Section 7 concludes the work.

2. Component Modeling

In this section, we develop the component modal equations of motion for a flexible payload-gripper system. Consider an arbitrary flexible payload grasped by an actuating robotic gripper as shown in Figure 1. To simplify the equations of motion of the system, a set of constraints are imposed to prevent the flexible payload from undergoing rigid-body motion with respect to the robot end-effector. For example, such constraints can be imposed on the flexible payload by maintaining a rigid connection (i.e., no actuator) in the gripper, as shown in Figure 1.

The undamped linear dynamic finite element model (FEM) of a flexible payload, subject to small deformation, is given by

$$\mathbf{M}\ddot{\mathbf{q}} + \mathbf{K}\mathbf{q} = \mathbf{f} \tag{1}$$

where $\mathbf{q}$ is the $n\times 1$ vector of nodal coordinates; $\mathbf{M}$ is the $n\times n$ mass matrix; $\mathbf{K}$ is the $n\times n$ stiffness matrix; $\mathbf{f}$ is the $n\times 1$ vector of external forces. In the following, a low-order representation of Eq. (1) is achieved using the CMS method.

2.1 Description of Component Mode Sets

The FEM of Eq. (1) can be partitioned as

$$\begin{bmatrix} \mathbf{M}_{rr} & \mathbf{M}_{ra} & \mathbf{M}_{ri} \\ \mathbf{M}_{ar} & \mathbf{M}_{aa} & \mathbf{M}_{ai} \\ \mathbf{M}_{ir} & \mathbf{M}_{ia} & \mathbf{M}_{ii} \end{bmatrix} \begin{bmatrix} \ddot{\mathbf{q}}_r \\ \ddot{\mathbf{q}}_a \\ \ddot{\mathbf{q}}_i \end{bmatrix} + \begin{bmatrix} \mathbf{K}_{rr} & \mathbf{K}_{ra} & \mathbf{K}_{ri} \\ \mathbf{K}_{ar} & \mathbf{K}_{aa} & \mathbf{K}_{ai} \\ \mathbf{K}_{ir} & \mathbf{K}_{ia} & \mathbf{K}_{ii} \end{bmatrix} \begin{bmatrix} \mathbf{q}_r \\ \mathbf{q}_a \\ \mathbf{q}_i \end{bmatrix} = \begin{bmatrix} \mathbf{f}_r \\ \mathbf{f}_a \\ \mathbf{f}_i \end{bmatrix} \tag{2}$$

where $\mathbf{q}_j = [\mathbf{q}_a^T \quad \mathbf{q}_r^T]$ and $\mathbf{q}_i$ represent the interface (or juncture) and interior nodal coordinates, respectively; the interface coordinates are divided into the constrained coordinates $\mathbf{q}_r$, which provides the rigid-body support of the payload, and the actuator coordinates $\mathbf{q}_a$, which defines those interface coordinates grasped by the actuators; $\mathbf{f}_j = [\mathbf{f}_a^T \quad \mathbf{f}_r^T]$ and $\mathbf{f}_i$ are the external forces acting on $\mathbf{q}_j$ and $\mathbf{q}_i$, respectively. Note that, without loss of generality, we can assume that $\mathbf{q}_a$ also represents the stroke lengths of the actuators. Using the CMS method, the nodal coordinates, $\mathbf{q}$, are represented in terms of generalized coordinates, $\mathbf{p}$, with the coordinate transformation

$$\mathbf{q} \approx \tilde{\mathbf{q}} = \mathbb{T}\mathbf{p} \tag{3}$$

where $\tilde{\mathbf{q}}$ represents the approximated nodal coordinates of $\mathbf{q}$; the component mode transformation matrix $\mathbf{T}$ is a matrix of pre-selected component modes. The definitions of these modes are described below.

Constraint Modes: A constraint mode [5] is defined as the static deformation shape that results by imposing a unit displacement on one of the actuator coordinates, while holding the remaining interface coordinates, $\mathbf{q}_j$, fixed. From this definition, the constraint modal matrix Ψ_c' is obtained by the following equation

$$\begin{bmatrix} \mathbf{K}_{rr} & \mathbf{K}_{ra} & \mathbf{K}_{ri} \\ \mathbf{K}_{ar} & \mathbf{K}_{aa} & \mathbf{K}_{ai} \\ \mathbf{K}_{ir} & \mathbf{K}_{ia} & \mathbf{K}_{ii} \end{bmatrix} \begin{bmatrix} \mathbf{0} \\ \mathbf{I}_{aa} \\ \Psi_c \end{bmatrix} = \begin{bmatrix} \mathbf{R}_{ra} \\ \mathbf{R}_{aa} \\ \mathbf{0} \end{bmatrix} \tag{4}$$

where $\mathbf{I}_{aa}$ is the identity matrix and $\mathbf{R}_{ra}$ represents the reaction forces at the $\mathbf{q}_r$ and $\mathbf{q}_a$ coordinates, respectively. Eq. (4) gives

$$\Psi_c' = \begin{bmatrix} \mathbf{0} \\ \mathbf{I}_{aa} \\ \Psi_c \end{bmatrix} = \begin{bmatrix} \mathbf{0} \\ \mathbf{I}_{aa} \\ -\mathbf{K}_{ii}^{-1}\mathbf{K}_{ia} \end{bmatrix} \tag{5}$$

Vibration Normal Modes: The $\mathbf{M}_{ii}$-normalized fixed-interface normal modal matrix Φ_n is obtained from the solution of the eigenproblem [6]:

$$\mathbf{M}_{ii}\Phi_n\Omega_n = \mathbf{K}_{ii}\Phi_n \tag{6}$$

in which

$$\Phi_n^T\mathbf{M}_{ii}\Phi_n = \mathbf{I}_{nn} \text{ and } \Phi_n^T\mathbf{K}_{ii}\Phi_n = \Omega_n \tag{7}$$

where $\mathbf{I}_{nn}$ is the identity matrix, $\Phi_n = [\varphi_1, \cdots, \varphi_{n_k}]$ in which φ_j is j^{th} normal mode and $\Omega_n = \text{diag}(\omega_{n_j}^2)$ is a diagonal matrix of natural frequencies ω_{n_j}, $j = 1, \ldots, n_k$; n_k represents the number of retained normal modes.

Quasi-Static Modes: A fixed-interface quasi-static modal matrix Φ_s is obtained from the solution of the eigenproblem:

$$\mathbf{K}_{ii}\Phi_s' = \Phi_s'\Omega_s \tag{8}$$

where $\Phi_s' = [\psi_1', \cdots, \psi_{n_s}']$ in which ψ_j' is j^{th} quasi-static mode and $\Omega_s = \text{diag}(\omega_{s_j}^2)$ is a diagonal matrix of quasi-static frequencies ω_{s_j}, $j = 1, \ldots, n_s$; n_s represents the number of retained static modes. Now, for computational efficiency, each static mode is orthogonalized with respect to the normal modes using the Gram-Schmidt procedure as follows:

$$\psi_j'' = \psi_j' - \sum_{m=1}^{n_k} \varphi_m^T \mathbf{M}_{ii} \psi_j' \varphi_m \quad (j = 1, \ldots, n_s) \tag{9}$$

Once ψ_j'' is found, it is normalized with respect to the mass matrix $\mathbf{M}_{ii}$ as follows:

$$\psi_j^T \mathbf{M}_{ii} \psi_j = 1 \tag{10}$$

Using the foregoing orthogonalization implies that $\varphi_m^T \mathbf{M}_{ii} \psi_j = 0$ or equivalently, $\Phi_n^T \mathbf{M}_{ii} \Phi_s = \mathbf{0}$. Finally, the static mode matrix in Eq. (8) is given as $\Phi_s = [\psi_1, \cdots, \psi_{n_s}]$.

2.2 Component Modal Model

Using the three types of modes described in the previous subsection, Eq. (1) can be rewritten in a component modal form. The coordinate transformation in Eq. (3) is given by

$$\begin{bmatrix} \mathbf{q}_a \\ \mathbf{q}_i \end{bmatrix} = \begin{bmatrix} \mathbf{I}_{aa} & \mathbf{0} & \mathbf{0} \\ \Psi_c & \Phi_n & \Phi_s \end{bmatrix} \begin{bmatrix} \mathbf{q}_a \\ \eta \\ \xi \end{bmatrix} = \mathbf{T}\mathbf{p} \tag{11}$$

where η and ξ are the normal and static modal coordinates, respectively. The component modal form of Eq. (1) is generated using the relations

$$\mathbf{M}_c = \mathbf{T}^T \mathbf{M}_r \mathbf{T}, \ \mathbf{K}_c = \mathbf{T}^T \mathbf{K}_r \mathbf{T}, \ \mathbf{f}_c = \mathbf{T}^T \mathbf{f}_r \tag{12}$$

where $\mathbf{M}_r$, $\mathbf{K}_r$ and $\mathbf{f}_r$ are the reduced matrices of Eq. (1) eliminating the elements corresponding to the constrained coordinates, $\mathbf{q}_r$. Eq. (12) yields the following equations of motion

$$\begin{bmatrix} \mathbf{M}_a & \mathbf{P}_n^T & \mathbf{P}_s^T \\ -\mathbf{P}_n & \mathbf{I} & \mathbf{0} \\ -\mathbf{P}_s & \mathbf{0} & \mathbf{I} \end{bmatrix} \begin{bmatrix} \ddot{\mathbf{q}}_a \\ \ddot{\eta} \\ \ddot{\xi} \end{bmatrix} + \begin{bmatrix} \mathbf{K}_a & \mathbf{0} & \mathbf{0} \\ \mathbf{0} & \Omega_n & \Lambda_n \\ \mathbf{0} & \Lambda_s & \Omega_s \end{bmatrix} \begin{bmatrix} \mathbf{q}_a \\ \eta \\ \xi \end{bmatrix} = \begin{bmatrix} \mathbf{f}_a + \Psi_c^T \mathbf{f}_i \\ \Phi_n^T \mathbf{f}_i \\ \Phi_s^T \mathbf{f}_i \end{bmatrix} \tag{13}$$

where:

$$\mathbf{M}_a = \mathbf{M}_{aa} + \mathbf{M}_{ai}\Psi_c + \Psi_c^T(\mathbf{M}_{ia} + \mathbf{M}_{ii}\Psi_c),$$
$$\mathbf{P}_n = -\Phi_n^T(\mathbf{M}_{ia} + \mathbf{M}_{ii}\Psi_c),$$
$$\mathbf{P}_s = -\Phi_s^T(\mathbf{M}_{ia} + \mathbf{M}_{ii}\Psi_c),$$
$$\mathbf{K}_a = \mathbf{K}_{aa} + \mathbf{K}_{ai}\Psi_c,$$
$$\Lambda_n = \Phi_n^T \mathbf{K}_{ii} \Phi_s \text{ and } \Lambda_s = \Phi_s^T \mathbf{K}_{ii} \Phi_n.$$

The top partition of Eq (13) governs the motion of the actuator coordinates and can be expressed in the form

$$\mathbf{M}_a \ddot{\mathbf{q}}_a + \mathbf{K}_a \mathbf{q}_a = \mathbf{f}_a + \Psi_c^T \mathbf{f}_i + \mathbf{P}_n^T \ddot{\eta} + \mathbf{P}_s^T \ddot{\xi} \tag{14}$$

The middle partition of Eq. (13) governs the response of the normal modal coordinates and is written as

$$\ddot{\eta} + \Omega_n \eta + \Lambda_n \xi = \mathbf{P}_n \ddot{\mathbf{q}}_a + \Phi_n^T \mathbf{f}_i \tag{15}$$

in which the term $\mathbf{P}_n \ddot{\mathbf{q}}_a$ represents an effective force acting on the normal modal coordinates due to the motion of the actuator coordinates. The matrix $\mathbf{P}_n$ is called a normal modal participation factor matrix [7], which represents the multiplication factor for the acceleration of the actuator coordinates. Similarly, the bottom partition in Eq. (13) governs the response of the quasi-static modal coordinates and is given by

$$\ddot{\xi} + \Omega_s \xi + \Lambda_s \eta = \mathbf{P}_s \ddot{\mathbf{q}}_a + \Phi_s^T \mathbf{f}_i \tag{16}$$

in which the term $\mathbf{P}_s \ddot{\mathbf{q}}_a$ represents the effective force acting on the static modal coordinates due to the motion of the constraint coordinates. Herein, the matrix $\mathbf{P}_s$ is named a quasi-static modal participation factor matrix.

3. Two-Time Scale Modeling

The system represented by Eq. (15) and Eq. (16) has $n_k + n_s$ DOF but only n_a actuator inputs (or n_s sensor outputs). If $n_k + n_s > n_a$, this poses significant limitations (i.e., uncontrollable or unobservable) for control design purposes, compared to the cases of static shape or vibration controls only. A viable solution is provided using a singular perturbation approach [8].

Define a perturbation parameter as $\mu = 1/\sqrt{k}$, where k is a scale factor which can be regarded as the smallest non-zero constant of Ω_n. It should be noted that the singular perturbation approach is valid for $\mu \ll 1$ [9]. Factoring $\Omega_n = (1/\mu)\Omega_k$, a new variable is defined as

$$\mathbf{z} = \frac{1}{\mu} \Omega_k \eta \tag{17}$$

Substituting the new variable into Eq. (14), (15) and (16) leads to

$$\ddot{\mathbf{q}}_a = \mathbf{M}_a^{-1}(-\mathbf{K}_a \mathbf{q}_a + \mu \mathbf{P}_n^T \Omega_k^{-1} \ddot{\mathbf{z}} + \mathbf{P}_s^T \ddot{\xi} + \mathbf{f}_a + \Psi_c^T \mathbf{f}_i) \tag{18a}$$

and

$$\mu \ddot{\mathbf{z}} = \Omega_k(-\mathbf{z} - \Lambda_n \xi + \mathbf{P}_n \ddot{\mathbf{q}}_a + \Phi_n^T \mathbf{f}_i) \tag{18b}$$

$$\ddot{\xi} = -\Omega_s \xi - \mu \Lambda_s \Omega_k^{-1} + \mathbf{P}_s \ddot{\mathbf{q}}_a + \Phi_s^T \mathbf{f}_i \tag{18c}$$

Now setting $\mu = 0$, the system exhibits quasi-static motions. Then, Eq. (18) degenerates into the slow subsystem

$$\ddot{\bar{\mathbf{q}}}_a = \mathbf{M}_a^{-1}(-\mathbf{K}_a\bar{\mathbf{q}}_a + \mathbf{P}_s^T\ddot{\bar{\boldsymbol{\xi}}} + \bar{\mathbf{f}}_a + \boldsymbol{\Psi}_c^T\bar{\mathbf{f}}_i) \quad (19a)$$

$$\bar{\mathbf{z}} = \boldsymbol{\Lambda}_n\boldsymbol{\xi} + \mathbf{P}_n\ddot{\bar{\mathbf{q}}}_a + \boldsymbol{\Phi}_n^T\bar{\mathbf{f}}_i \quad (19b)$$

$$\ddot{\boldsymbol{\xi}} = -\boldsymbol{\Omega}_s\boldsymbol{\xi} + \mathbf{P}_s\ddot{\bar{\mathbf{q}}}_a + \boldsymbol{\Phi}_s^T\bar{\mathbf{f}}_i \quad (19c)$$

where the overbars indicate that the corresponding quantities are evaluated in the slow time scale (i.e., $\mu = 0$): $\bar{\mathbf{f}}_i$ represents the quasi-static or slow-varying parts (i.e., gravity) of $\mathbf{f}_i$. Furthermore, by definition, a quasi-static problem can be described as having no time variations [10]. For example, eliminating any time-varying term in (Eq. 19c), we obtain

$$\boldsymbol{\xi} = \boldsymbol{\Omega}_s^{-1}\boldsymbol{\Phi}_s^T\bar{\mathbf{f}}_i \quad (20)$$

From this equation, note that the static modal coordinate $\boldsymbol{\xi}$ is not affected by an actuator command and, hence, cannot be controlled. Evaluating the bottom partition of Eq. (11) in the slow time scale yields

$$\bar{\mathbf{q}}_i = \boldsymbol{\Psi}_c\bar{\mathbf{q}}_a + \boldsymbol{\Phi}_s\boldsymbol{\xi} \quad (21)$$

Introducing a fast time scale as $\tau = t/\mu$ and defining the fast variable as $\tilde{\mathbf{z}} = \mathbf{z} - \bar{\mathbf{z}}$, $\ddot{\tilde{\mathbf{q}}}_a = \ddot{\mathbf{q}}_a + \ddot{\bar{\mathbf{q}}}_a$ and $\tilde{\mathbf{f}}_i = \mathbf{f}_i - \bar{\mathbf{f}}_i$, Eq. (18a) and (18b) become

$$\ddot{\tilde{\mathbf{q}}}_a = \mathbf{M}_a^{-1}(-\mathbf{K}_a\mathbf{q}_a + \mathbf{P}_n^T\boldsymbol{\Omega}_n^{-1}\frac{d^2\tilde{\mathbf{z}}}{d\tau^2} + \tilde{\mathbf{f}}_a + \boldsymbol{\Psi}_c^T\tilde{\mathbf{f}}_i) \quad (22a)$$

$$\frac{d^2\tilde{\mathbf{z}}}{d\tau^2} = \boldsymbol{\Omega}_k(-\tilde{\mathbf{z}} + \mathbf{P}_n\ddot{\tilde{\mathbf{q}}}_a + \boldsymbol{\Phi}_n^T\tilde{\mathbf{f}}_i) \quad (22b)$$

where the tildas indicate that the corresponding quantities are evaluated in the fast time scale. $\tilde{\mathbf{f}}_i$ represents the fast-varying parts of $\mathbf{f}_i$. Now substituting Eq. (22a) into Eq. (22b) the fast subsystem can be found to be

$$(\boldsymbol{\Omega}_k^{-1} - \mathbf{P}_n\mathbf{M}_a^{-1}\mathbf{P}_n^T\boldsymbol{\Omega}_n^{-1})\frac{d^2\tilde{\mathbf{z}}}{d\tau^2} = -\tilde{\mathbf{z}} - \mathbf{P}_n\mathbf{M}_a^{-1}\mathbf{K}_a\tilde{\mathbf{q}}_a + \mathbf{P}_n\mathbf{M}_a^{-1}\tilde{\mathbf{f}}_a + (\mathbf{P}_n\mathbf{M}_a^{-1}\boldsymbol{\Psi}_c^T + \boldsymbol{\Phi}_n^T)\tilde{\mathbf{f}}_i \quad (23)$$

4. Composite Modal Controller

In this section, we demonstrate the feasibility of solving the problem of composite static shape and vibration control of a flexible payload. On the basis of the above two-time scale model, represented by Eq. (21) and (23), a feedback controller for the flexible payload can be designed according to a composite control strategy [8].

If actuator displacements, $\mathbf{q}_a$, are commanded, the composite control divides the control input into two: one for static shape control and the other for vibration suppression, i.e., $\mathbf{q}_a = \bar{\mathbf{q}}_a + \tilde{\mathbf{q}}_a$, where $\bar{\mathbf{q}}_a$ is the static shape control input for the slow subsystem and $\tilde{\mathbf{q}}_a$ is the vibration control input for the fast subsystem. The shape control input $\tilde{\mathbf{q}}_a$ is designed with constraint $\tilde{\mathbf{q}}_a = \mathbf{0}$.

Now, let the static shape control input $\bar{\mathbf{q}}_a$ is set to the desired value $\bar{\mathbf{q}}_a^d$ in Eq. (21), and the result is

$$\bar{\mathbf{q}}_i^f - \bar{\mathbf{q}}_i = \boldsymbol{\Psi}_c(\bar{\mathbf{q}}_a^d - \bar{\mathbf{q}}_a) \quad (23)$$

where $\bar{\mathbf{q}}_i^f$ is the best-fit solution to the desired (steady-state) payload shape $\bar{\mathbf{q}}_i^d$, which can be obtained when $\bar{\mathbf{q}}_a^d$ is applied. This equation is solved for $\bar{\mathbf{q}}_i^f$, and is subtracted by $\bar{\mathbf{q}}_i^d$ from both sides, yielding

$$\bar{\mathbf{q}}_i^f - \bar{\mathbf{q}}_i^d = \boldsymbol{\Psi}_c(\bar{\mathbf{q}}_a^d - \bar{\mathbf{q}}_a) - (\bar{\mathbf{q}}_i^d - \bar{\mathbf{q}}_i) \quad (24)$$

To minimize $\left|\bar{\mathbf{q}}_i^f - \bar{\mathbf{q}}_i^d\right|$,

$$\boldsymbol{\Psi}_c(\bar{\mathbf{q}}_a^d - \bar{\mathbf{q}}_a) = (\bar{\mathbf{q}}_i^d - \bar{\mathbf{q}}_i) \quad (25)$$

Eq. (21) is substituted into the above equation to obtain

$$\bar{\mathbf{q}}_a^d = \boldsymbol{\Psi}_c^*(\bar{\mathbf{q}}_i^d - \boldsymbol{\Phi}_s\boldsymbol{\xi}) \quad (26)$$

where $\boldsymbol{\Psi}_c^*$ is the pseudo-inverse of $\boldsymbol{\Psi}_c$. This equation is the desired closed-loop feedback relation for the slow state.

Defining fast state vector as $\mathbf{x} = [\tilde{\mathbf{z}} \;\; d\tilde{\mathbf{z}}/d\tau]$ and multiplying the both sides of Eq, (23) by $\mathbf{M}_a\mathbf{P}_n^{-1}$, the state space representation given by

$$\dot{\mathbf{x}} = \tilde{\mathbf{D}}^{-1}\tilde{\mathbf{A}}'\mathbf{x} + \tilde{\mathbf{D}}^{-1}\tilde{\mathbf{B}}'\tilde{\mathbf{q}}_a = \tilde{\mathbf{A}}\mathbf{x} + \tilde{\mathbf{B}}\tilde{\mathbf{q}}_a \quad (27)$$

where:

$$\tilde{\mathbf{D}} = \begin{bmatrix} \mathbf{I} & \mathbf{0} \\ \mathbf{0} & \mathbf{M}_a\mathbf{P}_n^{-1}\boldsymbol{\Omega}_k^{-1} - \mathbf{P}_n^T\boldsymbol{\Omega}_n^{-1} \end{bmatrix}$$

$$\tilde{\mathbf{A}}' = \begin{bmatrix} \mathbf{0} & \mathbf{I} \\ -\mathbf{M}_a\mathbf{P}_n^{-1} & \mathbf{0} \end{bmatrix} \text{ and } \tilde{\mathbf{B}}' = \begin{bmatrix} \mathbf{0} \\ -\mathbf{K}_a \end{bmatrix}$$

Then vibration control can be provided by the LQR design method such that

$$\tilde{\mathbf{q}}_a = -\tilde{\mathbf{K}}\mathbf{x} \quad (28)$$

where $\tilde{\mathbf{K}}$ is a feedback gain matrix for the fast state.

5. Two-Time Scale Modal Estimator

Let's assume that the flexible payload is provided with n_m displacement sensors, which are mounted on the robot. Without loss of generality, let the sensor output measurement vector $\mathbf{y}$ be equal to the interior nodal displacements $\mathbf{q}_i$, i.e.,

$$\mathbf{y} = \mathbf{C}_o\mathbf{q}_i = \mathbf{C}_o(\boldsymbol{\Psi}_c\mathbf{q}_a + \boldsymbol{\Phi}_n\boldsymbol{\eta} + \boldsymbol{\Phi}_s\boldsymbol{\xi}) \quad (29)$$

where $\mathbf{C}_o$ is the sensor influence matrix. Substituting Eq. (17) into Eq. (29) leads to

$$\mathbf{y} = \mathbf{C}_o(\boldsymbol{\Psi}_c\mathbf{q}_a + \mu\boldsymbol{\Phi}_n\boldsymbol{\Omega}_k^{-1}\mathbf{z} + \boldsymbol{\Phi}_s\boldsymbol{\xi}) \quad (30)$$

in which $\mathbf{y}$ also consists of slow and fast parts, $\mathbf{y} = \tilde{\mathbf{y}} + \bar{\mathbf{y}}$ where:

$$\bar{\mathbf{y}} = \mathbf{C}_o(\Psi_c \bar{\mathbf{q}}_a + \Phi_s \xi) \tag{31a}$$

and

$$\begin{aligned}\tilde{\mathbf{y}} &= \mathbf{C}_o(\Psi_c \tilde{\mathbf{q}}_a + \Phi_n \Omega_n^{-1}\mathbf{z} + \Phi_s \xi) \\ &= \mathbf{C}_o \Psi_c \tilde{\mathbf{q}}_a + [\mathbf{C}_o \Phi_n \Omega_n^{-1} \quad \mathbf{0}]\mathbf{x} + [\mathbf{C}_o \Phi_s]\xi \\ &= \mathbf{C}_o \Psi_c \tilde{\mathbf{q}}_a + \tilde{\mathbf{C}}\mathbf{x} + \bar{\mathbf{C}}\xi\end{aligned} \tag{31b}$$

where ξ in Eq. (28b) is set as a constant.

Now, the problem of simultaneously estimating the fast states $\mathbf{x}$ and slow states ξ can be formulated by modifying a two-stage estimation technique [11]. Using this technique, two separate state estimators can be designed that simultaneously generate the estimates $\hat{\mathbf{x}}$ and $\hat{\xi}$ of $\mathbf{x}$ and ξ, respectively, from the same measurement output $\mathbf{y}$ in parallel computation. Let the fast state estimates, $\hat{\mathbf{x}}$, be expressed in the form

$$\hat{\mathbf{x}} = \hat{\mathbf{x}}' + \mathbf{V}\hat{\xi} \tag{32}$$

where $\hat{\mathbf{x}}'$ is the fast state estimate obtained as if there were no slow states present, i.e.,

$$\dot{\hat{\mathbf{x}}}' = \tilde{\mathbf{A}}\hat{\mathbf{x}}' + \tilde{\mathbf{B}}\ddot{\tilde{\mathbf{q}}}_a + \tilde{\mathbf{L}}(\mathbf{y} - \mathbf{C}_o \Psi_c \tilde{\mathbf{q}}_a - \tilde{\mathbf{C}}\hat{\mathbf{x}}') \tag{33}$$

where $\tilde{\mathbf{L}}$, which can be designed by the LQR method, is the Luenberger estimator gain chosen in such a way that $(\tilde{\mathbf{A}} - \tilde{\mathbf{L}}\tilde{\mathbf{C}}\hat{\mathbf{x}}')$ has negative real part poles, and

$$\dot{\hat{\xi}} = \bar{\mathbf{L}}[\mathbf{y} - \mathbf{C}_o \Psi_c \tilde{\mathbf{q}}_a - \tilde{\mathbf{C}}\hat{\mathbf{x}}' - (\tilde{\mathbf{C}}\mathbf{V} + \bar{\mathbf{C}})\hat{\xi}] \tag{34}$$

where the slow estimator gain $\bar{\mathbf{L}}$ is chosen such that the estimator given by Eq. (31) has the desired pole locations. The correction matrix, $\mathbf{V}$, is given by

$$\mathbf{V} = (\tilde{\mathbf{A}} - \tilde{\mathbf{L}}\tilde{\mathbf{C}})^{-1}\tilde{\mathbf{L}}\bar{\mathbf{C}} \tag{35}$$

Finally, the overall estimator gain can be obtained from

$$\mathbf{L} = \tilde{\mathbf{L}} + \mathbf{V}\bar{\mathbf{L}} \tag{36}$$

Using the above two-time scale estimator presented in this section, the estimates $\hat{\mathbf{x}}$ and $\hat{\xi}$ of $\mathbf{x}$ and ξ, respectively, can be obtained. Note that proofs are omitted due to space limitations.

6. Simulation Results

In this section, a numerical case study is developed to illustrate the effectiveness of the control design approach outlined in the previous sections. Simulations are carried out in MATLAB using the Runge-Kutta-Nystrom method for solving second order differential equations. As a representative example of flexible payloads, a flat, rectangular sheet metal part is chosen. The rectangular sheet metal plate is discretized via the finite element method using thin-plate finite elements. As shown in Figure 2, this plate is evenly divided into 25 nodes and 16 elements. Each node has 3 DOF: one out-of-plane displacement and two rotations. Node 13 is constrained through a rigid connection, to prevent the sheet metal plate from undergoing rigid-body motion with respect to the robot end-effector. Robotic gripper actuators are placed at nodes 7, 9, 17 and 19. Displacement sensors are located at nodes 1, 5, 21 and 25 in out-of-plane direction. The physical parameters of the sheet metal part, made of ANSI 304 steel, are shown in Table 1.

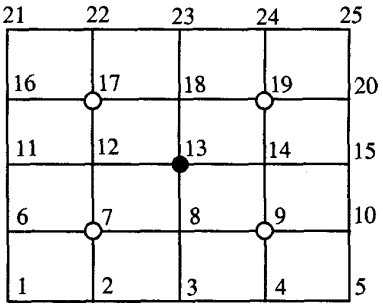

Fig. 2 Finite element mesh on sheet metal plate

Physical Parameters	Numerical values
Length	$1.0m$
Width	$0.8m$
Thickness	$0.001m$
Modulus of elasticity	$197Gpa$
Density	$8030kg/m^3$

Table 1 Physical parameters of sheet metal part

Mode No.	Normal Modes (Hz)	Quasi-static Modes (Hz)
1	5.8	0.31
2	8.4	0.41
3	9.7	0.43
4	9.9	0.45

Table 2 Normal and quasi-static modal parameters

The first four fixed-interface vibration normal mode and quasi-static mode frequencies are given in Table 2. These modes are retained in the modeling, and hence $n_k = n_s = 4$. In order to estimate and control $n_k + n_s$ (= 8) modes, at least the same number of actuators and sensors are desired. However, using the two-time scale approach, $n_a = n_m = 4$ actuators and sensors becomes sufficient. The perturbation parameter, $\mu = 0.0275$, which is small enough to separate the fast-time scale motions from the slow-time scale motions. Considering the target tolerance of an automotive body assembly, the goal of the shape control is to produce the steady-state deflection error within $\pm 0.5mm$.

For the fast-time scale subsystem, described by Eq. (22) and (28b), the system poles are shifted from the imaginary axis to the LHP (see Table 3) using the fast gains $\tilde{\mathbf{K}}$ and $\tilde{\mathbf{L}}$ designed by the LQR method. For the slow-time scale subsystem, the desired payload shape $\bar{\mathbf{q}}_i^d$ is set to zero. Then the desired "slow" actuator

displacement $\bar{\mathbf{q}}_a^d$ can be computed using the gains $\overline{\mathbf{K}}$ and $\overline{\mathbf{L}}$ obtained from Eq. (25) and (31), respectively.

Open-loop Poles	Closed-loop poles
$0 \pm 1j$	$-0.16 \pm 1.03j$
$0 \pm 1.44j$	$-1.69 \pm 1.09j$
$0 \pm 1.70j$	$-1.29 \pm 1.39j$
$0 \pm 1.68j$	$-1.56 \pm 0.97j$

Table 3 Physical parameters of sheet metal part

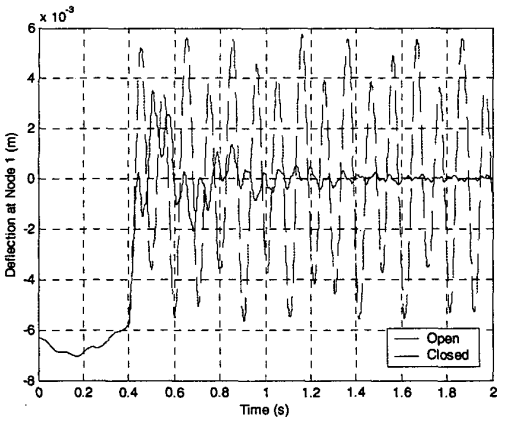

Fig. 3 Deflection profile at Node 1

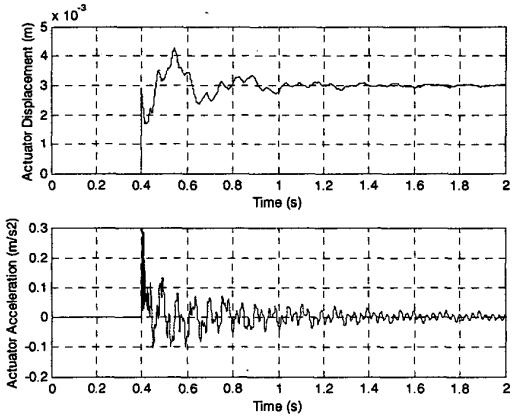

Fig. 4 Node 7 actuator displacement/acceleration profile

In this case study, static gravity and sinusoidal ($10Hz$) dynamic forces are continuously exerted on the sheet metal part as external disturbances. In addition, it is assumed that the sheet metal part is stationary after having reached a desired assembly location, and it is also tilted at an angle of 45 degrees from the vertical. Also, the actuators are initially fixed at zero position. The composite controller and the actuators are activated at t = $0.4sec$. Figure 3 shows the deflection profile at Node 1. As the figure shows, the initial static deflection ($\sim 6mm$) is corrected and the vibration is damped out effectively, Note that "open" corresponds to the open-loop static shape deformation controller, which excites vibration. Figure 4 shows the actuator displacement and acceleration profiles at Node 7 for the closed-loop control. The simulation results show that the proposed control design approach simultaneously corrects static shape deformation and suppresses vibration in the payload within the assembly tolerance of $\pm 0.5mm$.

7. Conclusion

A two-time scale approach has been developed for the simultaneous control of static shape deformation and vibration of flexible payloads grasped by an actuated gripper. The design of a composite control and a two-time scale estimator is presented. Simulation results demonstrate the effectiveness of the proposed control approach to counteract static and dynamic external disturbances. The work presented here is a part of on-going research, which is the development of a near-practice robotic assembly technology for automotive sheet metal parts [1]. The proposed controller and estimator will be applied to an experimental test-bed, which is currently under development [12].

References

1 Mills, J.K. and Ing, J., "Dynamic Modeling and Control of a Multi-Robot System for Assembly of Flexible Payloads with Application to Automotive Body Assembly," *J. of Robotic Systems*, 13(12), pp. 817-836, 1996.

2 Craig, R.R., Jr., "Substructure Methods in Vibration," *J. of Mechanical Design*, 117, pp. 207-213. 1995.

3 Wu, H.T. and Mani, N.K., "Modeling of Flexible Bodies for Multibody Dynamic Systems Using Ritz Vectors," *J. of Mechanical Design*, 116, pp. 437-444, 1994.

4 Yoo, W.S. and Haug, E.J., "Dynamics of Articulated Structures, Part I: Theory," *J. of Struc. Mechanics*, 14(1), pp. 105-126, 1986.

5 Hurty, W.C., " Dynamic Analysis of Structural Systems Using Component Modes," *AIAA Journal*, 3(4), pp.678-685, April 1965.

6 Craig, R.R., Jr., *Structural Dynamics: An Introduction to Computer Methods*, Wiley, New York, 1981.

7 Kammer, D.C. and Triller, M.J., "Selection of Component Modes for Craig-Bampton Substructure Representations," *J. of Vibration and Acoustics*, 118, pp. 264-270, 1996.

8 Kokotovic, P.V., Khalil, H.K., and O'Reilly, J., *Singularly Perturbed Methods in Control: Analysis and Design*, Academic Press, London, 1986.

9 Siciliano, B., Prasad, J.V.R., and Calise, A.J., "Output Feedback Two-Time Scale Control of Multilink Flexible Arms," *J. of Dyn. Systems, Measurement, and Control*, 114, pp. 70-77, 1992.

10 Balas, M.J., "Optimal Quasi-Static Shape Control for Large Aerospace Antennae," *J. of Optimization Theory and Applications*, 46(2), pp. 153-170, June 1985.

11 Friedland, B., *Control Systems Design*, McGraw Hill Inc., 1986.

12 Park, E.J. and Mills, J.K., "Dynamic Modeling of Flexible Payloads Grasped by Actuated Grippers Using Component Mode Synthesis," To appear in *IEEE ICRA 2002*, Washington, D.C., May 11-15, 2001.